Yang *et al. Biochar* (2026) 8:136
https://doi.org/10.1007/s42773-026-00645-5

Biochar

ORIGINAL RESEARCH Open Access

Long-term biochar amendment increased dissimilatory nitrate reduction to ammonium concomitantly suppressing denitrification and anaerobic ammonium oxidation in deep alkaline paddy soil

Qiannan Yang[1], Guilong Zhang[1,2,3], Jie Li[1], Hu Li[4], Lukas Van Zwieten[5] and Lili Wang[1*]

Abstract

Dissimilatory nitrate reduction to ammonium (DNRA) conserves soil nitrogen (N), whereas denitrification and anaerobic ammonium oxidation (anammox) can result in soil N loss. Despite biochar's potential to modulate N cycling pathways, its effects on dissimilatory nitrate reduction in alkaline paddy soils remain poorly characterized. Using ^{15}N tracer pairing techniques in soil slurries, we quantified denitrification, anammox, and DNRA rates in soils to 80 cm depth that had received surface annual application of 0.05 t/ha of rice straw biochar. We then partitioned nitrate reduction pathways and identified associated microbial communities. Denitrification showed the greatest variability in rates, proportional contribution and community composition, indicating its dominant role in partitioning nitrate reduction pathways in both surface and deep layers. Random forest and structural equation modeling identified the edaphic factors of soil pH, SOC/NO_3^- ratio, and Fe^{2+} concentration as key drivers. In surface layers, biochar amendment optimized these parameters, stimulating both denitrification and DNRA rates. In deep layers, however, biochar progressively elevated pH above optimal thresholds and lowered SOC/NO_3^- ratio, further suppressing *napA* gene abundance and denitrification rates while increasing DNRA rates and proportions. Our findings demonstrate that long-term biochar amendment promotes DNRA and suppresses denitrification and anammox in deep alkaline paddy soil. These results provide mechanistic evidence for biochar's role in conserving soil N through depth-dependent modulation of microbial N cycling pathways in alkaline paddy systems.

Highlights

- DNRA dominates over denitrification with increasing depths.
- Long-term biochar amendment promotes DNRA whereas suppresses denitrification and anammox in deep alkaline paddy soil.
- The trade-off between denitrification and DNRA was mediated by *napA*, *nosZ* and denitrifiers via pH, SOC/NO_3^-, and Fe^{2+}.
- Our findings emphasize the role of biochar in regulating dissimilatory nitrate reduction in alkaline deep paddy soil.

*Correspondence:
Lili Wang
lili0229ok@126.com
Full list of author information is available at the end of the article

Springer

Keywords Denitrification, DNRA, Rice straw biochar, Deep soil

Graphical Abstract

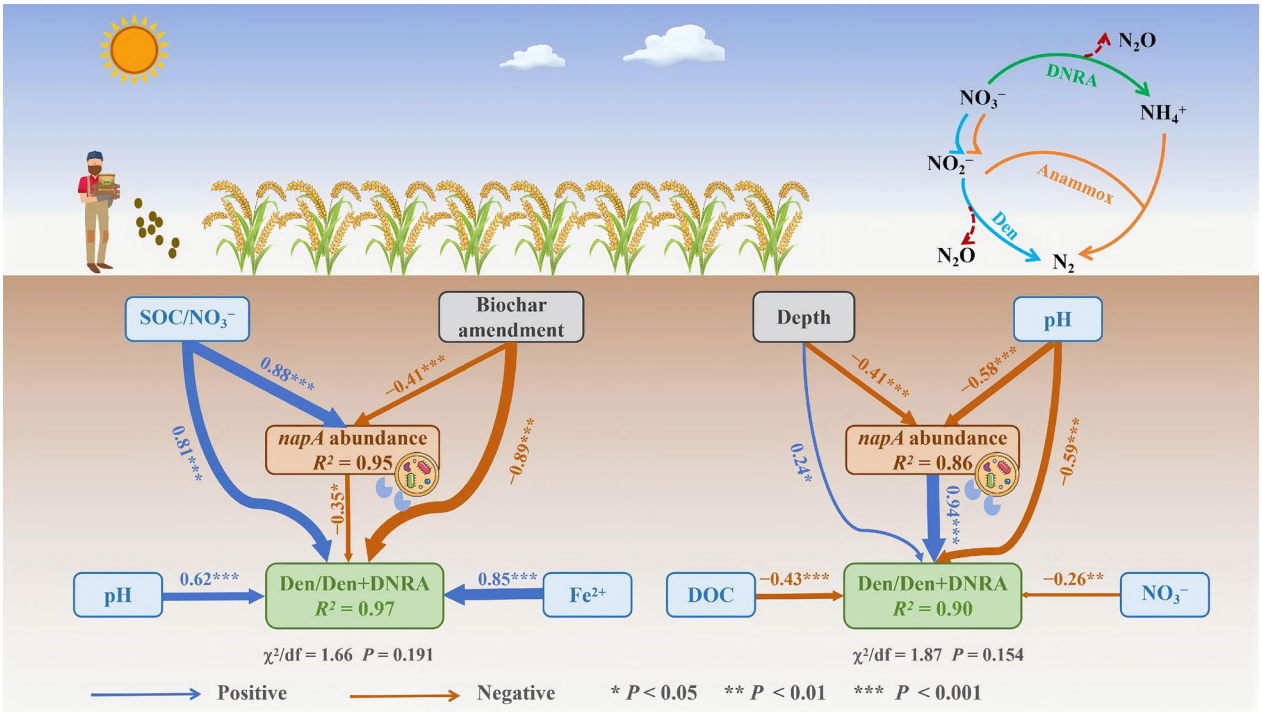

1 Introduction

The dissimilatory nitrate reduction process in paddy soils constitutes a vital component of the nitrogen (N) cycle, including denitrification, anammox, and dissimilatory nitrate reduction to ammonium (DNRA). Denitrification represents the primary N loss pathway in paddy soils, with the highest activity in the topsoil layer, with rates reaching 2.19 ± 0.39 mg N kg^{-1} d^{-1} (Ding et al. 2021). The anammox process occurs in the surface soil layer, with a rate of 1.13 ± 0.16 mg N kg^{-1} d^{-1}. In contrast, DNRA can reduce nitrate to ammonium, which contributes to lower N loss, thus conserving plant available N (Shan et al. 2016; Zhang et al. 2021). The interactions between denitrification, anammox, and DNRA not only influence N transformation and loss but also significantly impact greenhouse gas emissions and soil health. Recent publications on factors affecting nitrate dissimilatory reduction processes in paddy soils indicate that soil pH, C/N ratio, inorganic N content, and redox conditions are key regulators of these processes, but these studies focus on acidic paddy topsoil (Li et al. 2020a, b; Cheng et al. 2022). However, the controlling factors of dissimilatory nitrate reduction process in alkaline paddy soils, especially in deep layers, still remain unclear.

Biochar amendment to paddy fields exerts significant effects on dissimilatory nitrate reduction by regulating microbial activity and soil physicochemical properties (Joseph et al. 2015), particularly through competitive and synergistic interactions between denitrification and DNRA. When soil has a low C/NO_3^- ratio, denitrification is typically dominant because denitrifying bacteria exhibit higher affinity for nitrate (Jia et al. 2020). In turn, under high C/NO_3^- conditions, biochar amendment can promote DNRA over denitrification process, thereby lowering N loss and increasing soil NH_4^+ retention (Wei et al. 2022). Denitrification and DNRA process also exhibit synergistic relations under biochar amendment due to (1) regulation of soil pH: biochar can elevate soil pH, thus favoring *nosZ* gene expression in acidic soils, but it also enhances the activity of DNRA-associated microorganisms (Zhang et al. 2022a, b; Gao et al. 2025); (2) organic carbon supply: biochar increases dissolved organic carbon (DOC) content in soil, providing additional electron donors for DNRA (He et al. 2019;

Zhang et al. 2022a, b); (3) alteration of microbial communities: biochar enhances DNRA rates and reduces soil N_2O emissions by increasing the abundance of specific microorganisms (Wei et al. 2022). The trade-offs between denitrification and DNRA are likely to be significantly different in acidic and alkaline soils. However, most of these mechanisms are applicable to acidic surface paddy soils (Pandey et al. 2019; Li et al. 2020a). As the percolation and accumulation effects of NO_3^- in deeper paddy soil become increasingly evident, N loss is becoming increasingly severe especially in acidic soils (Ding et al. 2021). It is unclear whether biochar amendment exerts a competitive or synergistic effect on regulating denitrification and DNRA in deep alkaline paddy soil, and the relevant mechanisms have not yet been revealed.

This study aims to investigate the microbial regulatory mechanisms of dissimilatory nitrate reduction processes in deep alkaline (pH > 8) paddy soil under long-term biochar amendment, thereby addressing the gaps in previous research. The specific objectives of this study were to: (1) quantify how long-term biochar amendment affects denitrification, anammox, and DNRA rates of different depths in alkaline paddy soil; (2) assess the physicochemical and microbial drivers under biochar amendment in soils of different depths; (3) elucidate the microbial mechanisms underlying these effects. This work aims to provide mechanistic insights into long-term biochar amendment–depth–microbe interactions, contributing to a deeper understanding of how biochar can be used to regulate dissimilatory nitrate reduction processes in deep alkaline paddy soil, and providing guidance for tailoring biochar strategies to alkaline soil environments.

2 Materials and methods

2.1 Study sites and soil sampling

This study was initiated in 2019, and long-term (> 5 year) biochar amendment was performed in the paddy soil in Ninghe, Tianjin (39.47° N,117.70° E). Biochar was mixed thoroughly and spread evenly on the surface layer of the paddy soil at an annual application rate of of 0.05 t ha^{-1} yr^{-1} of rice straw. We used a rotary tiller to incorporate it into the tillage layer (0–40 cm) and repeated this process 1–2 times to ensure uniform distribution to deeper layers. The biochar used in the incubation study was made from rice straw, which was pyrolyzed in a muffle furnace at a temperature of 500 ℃ (with a heating rate of 5 ℃ min^{-1}) for 8 h under oxygen limited conditions. Detailed information on the biochar properties is listed in Table S1 and Fig. S1.

The collected paddy soil belongs to Eutric Cambisols, which were developed from a sandy loam deposit and calcium carbonate was deposited at the bottom due to the groundwater. Paddy soils from the 0–20, 20–40, 40–60, and 60–80 cm layers were collected from the control (CK) and biochar amended (BC) plots, respectively. The soil samples were collected following the harvest of rice in 2024 from 5 locations within the plots. Each sample was divided into three parts: (1) one subsample was processed for physicochemical analysis; (2) the second subsample was stored at 4 ℃ for the determination of the potential rates of denitrification, anammox, and DNRA rate within three days after sampling from the field soil; (3) the third subsample was stored at − 80 ℃ for molecular analysis. Unless otherwise stated, the following measurements were performed in triplicate.

2.2 Soil physicochemical properties analysis

Soil pH and electrical conductivity (EC) were determined using soil to water ratios of 1:2.5 and 1:5, respectively. Soil total carbon (TC) and total nitrogen (TN) were determined using an elemental analyzer (Elementar analyzer vario MaxCNOHS, Germany). Soil organic carbon (SOC) content was determined by the wet oxidation method with $K_2Cr_2O_7$ after removing carbonate using hydrochloric acid (HCl) (Bao 2000). Soil dissolved organic carbon (DOC) content was determined using a TOC analyzer (Elementar, Germany). Soil NH_4^+–N and NO_3^-–N concentrations were extracted with 2 M KCl solution at a soil/solution ratio of 1:5 (weight/volume). The KCl extracts were then filtered through filter paper, and the concentrations of NH_4^+–N and NO_3^-–N in the extracts were determined by a continuous-flow analyzer (Smartchem 200S/N1104238, WESTCO, France) (Yin et al. 2017). Soil available phosphorus (AP) was measured by the molybdenum-blue method. Fe^{2+} in soils was extracted by 5 mL 0.5 mol L^{-1} HCl. The contents of Fe^{2+} in the extractions were determined using a spectrophotometer (Li et al. 2020a). The soil physicochemical properties are presented in Table 1.

2.3 Measuring potential rates of denitrification, anammox, and DNRA

The rates of denitrification, anammox, and DNRA were simultaneously measured using a soil slurry-based ^{15}N tracer pairing technique and membrane inlet mass spectrometry (MIMS, Bay Instruments, Easton, MD, USA) (Hou et al. 2012; Liu et al. 2019). Briefly, fresh soil samples were homogenized by hand mixing in an anaerobic glove box at a volume ratio of 1:7 (soil/water) and transferred into individual 160 mL serum bottles. Each sample was wrapped with aluminum foil to keep the incubation bottles dark. The system used a multichannel peristaltic pump that maintained a consistent flow of 1.0–1.4 mL min^{-1}, and the paddy soil core with inlet tubing and outlet tubing. The bottom water enriched with ^{15}N–NO_3^- (90–99% ^{15}N-KNO_3) to final

Table 1 Soil physicochemical characteristics in the control and biochar amendment (BC) in different depths of the paddy soil

Depth (cm)	Treatment	pH	EC (ms cm^{-1})	TC (g kg^{-1})	SOC (g kg^{-1})	DOC (mg kg^{-1})	TN (g kg^{-1})	NH_4^+-N (mg kg^{-1})
0–20	Control	6.81 ± 0.07a	488.0 ± 10.4a	12.84 ± 0.04a	3.801 ± 0.052a	21.76 ± 0.62a	1.064 ± 0.014a	8.164 ± 0.190a
	BC	7.43 ± 0.05b	334.33 ± 8.50b	19.30 ± 0.04b	3.435 ± 0.023b	16.17 ± 0.42b	0.855 ± 0.017b	7.871 ± 0.120a
20–40	Control	7.20 ± 0.08a	474.00 ± 11.14a	11.46 ± 0.02a	3.587 ± 0.058a	25.56 ± 0.14a	0.994 ± 0.008a	11.427 ± 0.292a
	BC	7.94 ± 0.02b	310.67 ± 2.08b	17.82 ± 0.08b	2.969 ± 0.047b	17.74 ± 0.27b	0.345 ± 0.016b	6.003 ± 0.075b
40–60	Control	7.59 ± 0.04a	455.00 ± 13.08a	9.43 ± 0.02a	2.124 ± 0.064a	17.02 ± 0.24a	0.517 ± 0.008a	6.872 ± 0.248a
	BC	8.00 ± 0.05b	300.33 ± 2.52b	13.41 ± 0.06b	1.316 ± 0.001b	15.17 ± 0.80b	0.209 ± 0.002b	5.597 ± 0.079b
60–80	Control	7.88 ± 0.07a	331.67 ± 2.52a	9.24 ± 0.03a	1.243 ± 0.017a	13.79 ± 0.61a	0.220 ± 0.007	5.954 ± 0.088a
	BC	8.10 ± 0.02b	286.00 ± 2.65b	10.07 ± 0.06b	1.101 ± 0.005b	11.10 ± 0.22b	0.190 ± 0.001b	5.330 ± 0.038b
Two-way ANOVA								
D		291.376**	190.868**	22,665.759**	5149.461**	420.251**	5616.594**	463.106**
B		507.430**	1604.733**	51,180.937**	856.089**	543.521**	4468.785**	797.459**
D × B		27.665**	75.070**	4602.947**	77.515**	50.740**	850.658**	312.033**
Depth (cm)	**Treatment**	**NO_3^-–N (mg kg^{-1})**	**AP (mg kg^{-1})**	**TC/TN (%)**	**C/NO_3^- (× 10^3)**	**SOC/NO_3^- (× 10^3)**	**DOC/NO_3^- (%)**	**Fe^{2+} (mg g^{-1})**
0–20	Control	9.392 ± 0.098a	15.47 ± 0.47a	12.07 ± 0.12a	1.367 ± 0.010a	404.72 ± 5.72a	2.317 ± 0.048a	0.300 ± 0.0009a
	BC	8.058 ± 0.079b	20.60 ± 0.68b	22.57 ± 0.41b	2.395 ± 0.021b	515.71 ± 0.91b	2.007 ± 0.033b	0.315 ± 0.0003b
20–40	Control	6.660 ± 0.044a	14.15 ± 0.03a	11.53 ± 0.09a	1.721 ± 0.009a	365.81 ± 3.91a	3.837 ± 0.006a	0.273 ± 0.0038a
	BC	6.984 ± 0.041b	8.28 ± 0.13b	51.69 ± 2.11b	2.552 ± 0.005b	345.78 ± 2.02b	2.540 ± 0.024b	0.147 ± 0.0034b
40–60	Control	9.804 ± 0.055a	6.25 ± 0.11a	18.25 ± 0.24a	0.962 ± 0.003a	263.60 ± 6.81a	1.735 ± 0.015a	0.141 ± 0.0006a
	BC	7.630 ± 0.049b	7.50 ± 0.10b	64.17 ± 0.48b	1.758 ± 0.006b	188.44 ± 0.96b	1.988 ± 0.094b	0.153 ± 0.0013b
60–80	Control	8.585 ± 0.109a	4.04 ± 0.14a	42.10 ± 1.27a	1.076 ± 0.011a	162.88 ± 1.60a	1.606 ± 0.058a	0.103 ± 0.0023a
	BC	8.125 ± 0.062b	6.27 ± 0.08b	52.93 ± 0.14b	1.239 ± 0.002b	135.49 ± 0.44b	1.366 ± 0.017b	0.119 ± 0.0013b
Two-way ANOVA								
D		961.644**	2127.228**	1259.849**	12,074.670**	8858.365**	1508.960**	9936.105**
B		975.588**	30.279**	5263.278**	29,195.309**	3.911ns	449.799**	577.909**
D × B		342.886**	352.100**	647.593**	2065.486**	741.772**	298.707**	1622.620**

Data are expressed as the mean ± standard deviation ($n = 3$); Different letters represent the significance between control and BC treatment in different depths of the paddy soil according to two-way ANOVA ($P < 0.05$)

TC soil total carbon, *SOC* soil organic carbon, *DOC* soil dissolved organic carbon, *TN* soil total nitrogen, *AP* soil available phosphorus, *AK* soil available potassium, *D* Depth effect, *B* biochar (BC) treatment

concentrations of 100 μM $^{15}N–NO_3^-$ and kept at near in situ temperature. Following an overnight pre-incubation to allow the system to reach equilibrium (McTigue et al. 2016), inlet and outlet samples were collected once every 6 h for 24 h with 12 mL gas-tight vials (Exetainer, Labco). Immediately after collection, 200 μL of 50% $ZnCl_2$ solution was added to each sample to inhibit microbial activity. All vials were sealed with butyl rubber septa and stored underwater at 4 °C until analysis. Potential denitrification, anammox, and DNRA rates in the slurries were quantified by measuring process-specific ^{15}N-labeled products. The concentrations of $^{29}N_2$ and $^{30}N_2$ in the vials were measured by membrane inlet mass spectrometry (MIMS), and the potential denitrification, anammox, and DNRA rates were calculated by the $^{29}N_2$ and $^{30}N_2$ production and $^{15}NH_4^+$ during the incubation period, as described in Table S2.

2.4 Soil DNA extraction and quantitative PCR assay

Total DNA in the soil sub-samples was extracted using the PowerSoil DNA Kit (QIAGEN, USA) according to the manufacturer's instructions. The concentration and purity of the extracted DNA was assessed with a NanoDrop spectrophotometer (Thermo Fisher Scientific, Wilmington, USA). Real-time quantitative PCR was performed to quantify the abundance of nitrate reduction-related genes. The primers for the nitrate reduction-related genes were 3F/3R for *napA*, $F_{1a}CuF/R_3CuR$ for *nirK*, cd3aF/R3cd for *nirS*, and ZF/ZR for *nosZ*. The *nrfA* gene for DNRA and *hzs* gene for anammox were not detected in the samples, probably due to the high soil pH. Details of the primers used for each gene and the thermocycling conditions are listed in Table S3. The amplification efficiencies of the qPCR results were 90–110%, and the correlation coefficients (R^2) were higher than 0.98.

2.5 High-throughput sequencing

The purified products of *nirK*, *nirS*, and *nosZ* genes were sent for high-throughput sequencing using the Illumina MiSeq platform (Illumina, San Diego, CA, USA) according to the standard protocols of Majorbio BioPharm Technology Co. Ltd. (Shanghai, China). The quality sequences were binned into operational taxonomic units (OTUs) defined at the 97% similarity level using the UCLUST program (Edgar 2010) after chimera sequences were removed using Quantitative Insights Into Microbial Ecology (QIIME) (Caporaso et al. 2010). We deposited the raw reads of the *nirK*, *nirS*, and *nosZ* genes into the NCBI Sequence Read Archive (SRA) database under accession numbers PRJNA1441227, PRJNA1441200, and PRJNA1441235, respectively. Specifically, the relative abundance of specific orders encoded by *nirK*, *nirS*, and *nosZ* genes was calculated based on the composition of nitrate reducer communities in each treatment.

2.6 Statistical analysis

A two-way analysis of variance (ANOVA) was conducted to assess the effects of biochar amendment, soil depth, and their interaction on measured variables. Post hoc comparisons were performed using Duncan's multiple range test at a significance level ($P < 0.05$). All statistical analyses were carried out using IBM SPSS Statistics 27.0 (SPSS Inc., Armonk, NY, USA), evaluating differences in soil physicochemical properties, N transformation rates (denitrification, anammox, and DNRA), and copy numbers of nitrate reduction-related genes. The matrix-weighted UniFrac distance-based principal coordinate analysis (PCoA) was conducted using 'vegan' and 'ape' packages in R (version 4.3.1) to evaluate the microbial community compositions associated with denitrification, and the significance was simultaneously estimated by the permutation analysis of variance (PERMANOVA) test. The Circos package was used to visualize the distribution of the most abundant denitrification phyla (> 1%). The properties and images of the network were calculated and generated using the igraph package in R (Csárdi and Nepusz 2006) and Gephi (http://gephi.github.io/). Pearson correlation analyses between N transformation rates, functional gene abundances, and soil properties, as well as Mantel tests assessing relationships between denitrifier community composition and soil variables, were performed using the *vegan* package in R (version 4.3.1). The structural equation modeling (SEM) was performed with the lavaan package in R (version 4.3.1). The chi square test ($\chi 2$), comparative fit index (CFI), and standardized root mean square residual (SRMR) were used to assess the model fit.

3 Results

3.1 Depth-related patterns of denitrification, anammox, and DNRA in biochar-amended paddy soils

Both depth and biochar amendment, as well as their interaction effect, significantly influenced dissimilatory nitrate reduction in both surface and deep layers of paddy soils (Fig. 1). DNRA, denitrification, and anammox rates all exhibited a decreasing trend with increasing depth (Fig. 1a–c). With increasing depth, the relative contributions of DNRA and denitrification exhibited opposite trends. Overall, DNRA rates ranged from 5.03 to 17.90 nmol g^{-1} h^{-1} (Fig. 1a) and the proportion of DNRA significantly increased from 25.7% to 91.1% (Fig. 1d). Concomitantly, denitrification rates ranged from 1.23 to 37.86 nmol g^{-1} h^{-1} (Fig. 1b) and the proportion of denitrification significantly decreased from 67.9% to 7.2% (Fig. 1d). Anammox rates varied from 0.32 to 13.85 nmol g^{-1} h^{-1} (Fig. 1c) and their proportion also decreased from 23.5% to 1.9% (Fig. 1d).

BC treatment significantly increased the rates of DNRA, denitrification, and anammox in the surface layers of the paddy soil profile (Fig. 1a–c). Compared to control (CK) treatment, BC treatment significantly increased the proportion of denitrification in the surface layer (0–20 cm) by 6.2%, but decreased the proportion by 28.8% in the 20–40 cm layer, 17.8% in the 40–60 cm layer, and 27.8% in the 60–80 cm layer, respectively (Fig. 1d). BC treatment in turn decreased DNRA proportion by 2.9% in the 0–20 cm layer but increased DNRA proportion by 31.4% in the 20–40 cm layer, 22.2% in the 40–60 cm layer, and 37.0% in the 60–80 cm layer, respectively (Fig. 1d), which reached peak in the 60–80 cm layer. The denitrification/denitrification + DNRA ratio (Den/Den + DNRA) increased in the 0–20 cm layer by 5.2% but decreased by 33.9% in the 20–40 cm layer, 21.6% in the 40–60 cm layer, and 31.8% in the 60–80 cm layer under BC treatment (Fig. 1d). The proportion of anammox decreased in all depths, with the reduction of 3.8% in the surface layer, 2.7% in the 20–40 cm layer, 4.8% in the 40–60 cm layer, and 9.4% in the 60–80 cm layer under BC treatment, and decreased most in the 60–80 cm layer (Fig. 1d).

3.2 Vertical distribution of nitrate reduction-related gene abundance in biochar-amended paddy soils

The abundance of nitrate-reducing functional genes was quantified under BC treatment in different soil layers. The functional genes including *napA* and denitrification-related genes *nirK*, *nirS*, and *nosZ* were detected. The abundances of *nrfA* and *hzs* genes were too low to be detected. This may be attributed to the high alkaline soil pH, coupled with low oxygen and organic carbon

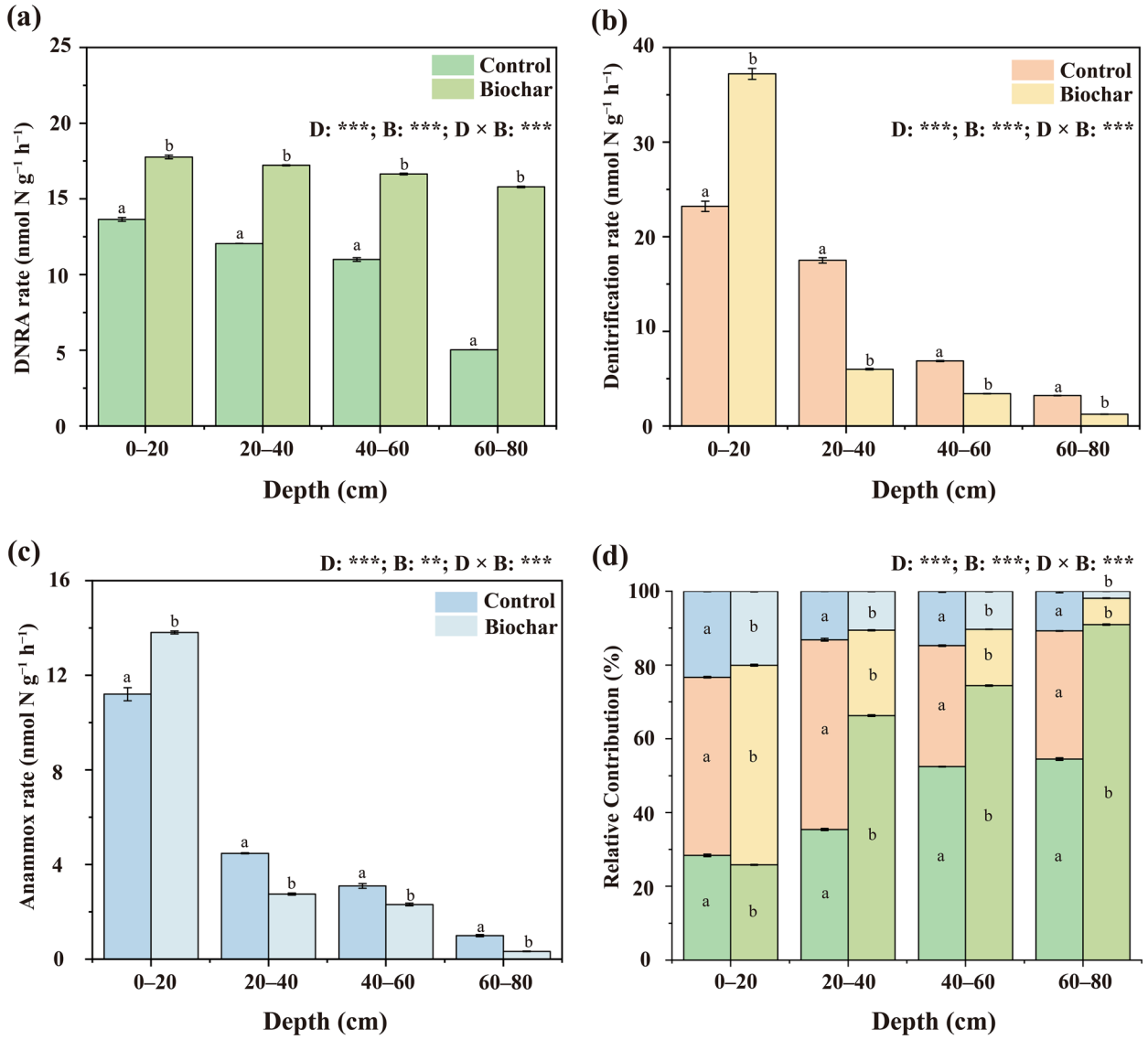

Fig. 1 Rates of DNRA (**a**), denitrification (**b**), and anammox (**c**), and their relative contributions (%) in control and biochar-amended (BC) treatments across different soil depths in paddy soil. Error bars show the standard deviation of each treatment ($n = 3$). Different letters indicate significant differences at $P < 0.05$. The effects of sampling depth (D), biochar amendment (B), and their interaction (D × B) in each soil are shown. *$P < 0.05$; **$P < 0.01$; ***$P < 0.001$

levels resulting from periodic drainage and increasing depth, suppressing microbial community activity associated with these functional genes. Overall, the nitrate reduction gene abundance ($\log_{10}$ copies) significantly decreased from 8.20 to −0.07 with increasing soil depth (Fig. 2), indicating deeper soil layers inhibited microbial activity. The *napA* gene ($\log_{10}$ copies) exhibited the most pronounced decreasing trend along the profile from 6.06 to 1.05 (Fig. 2c). The abundances of *nirS* (Fig. 2b) and *nosZ* (Fig. 2d) peaked within the 0–40 cm soil layer, consistent with the adaptation of denitrifying bacteria to microaerobic conditions.

BC treatment showed diametrically opposed effects on nitrate reduction functional gene abundance ($\log_{10}$ copies) in the surface and deep soil layers (Fig. 2). BC treatment significantly increased denitrification-related gene abundances (Fig. 2a, b, d) but reduced *napA* gene abundance in the 0–20 cm soil layer (Fig. 2c). This aligns with the changes of DNRA and denitrification rates in the surface layer. In contrast, BC treatment significantly

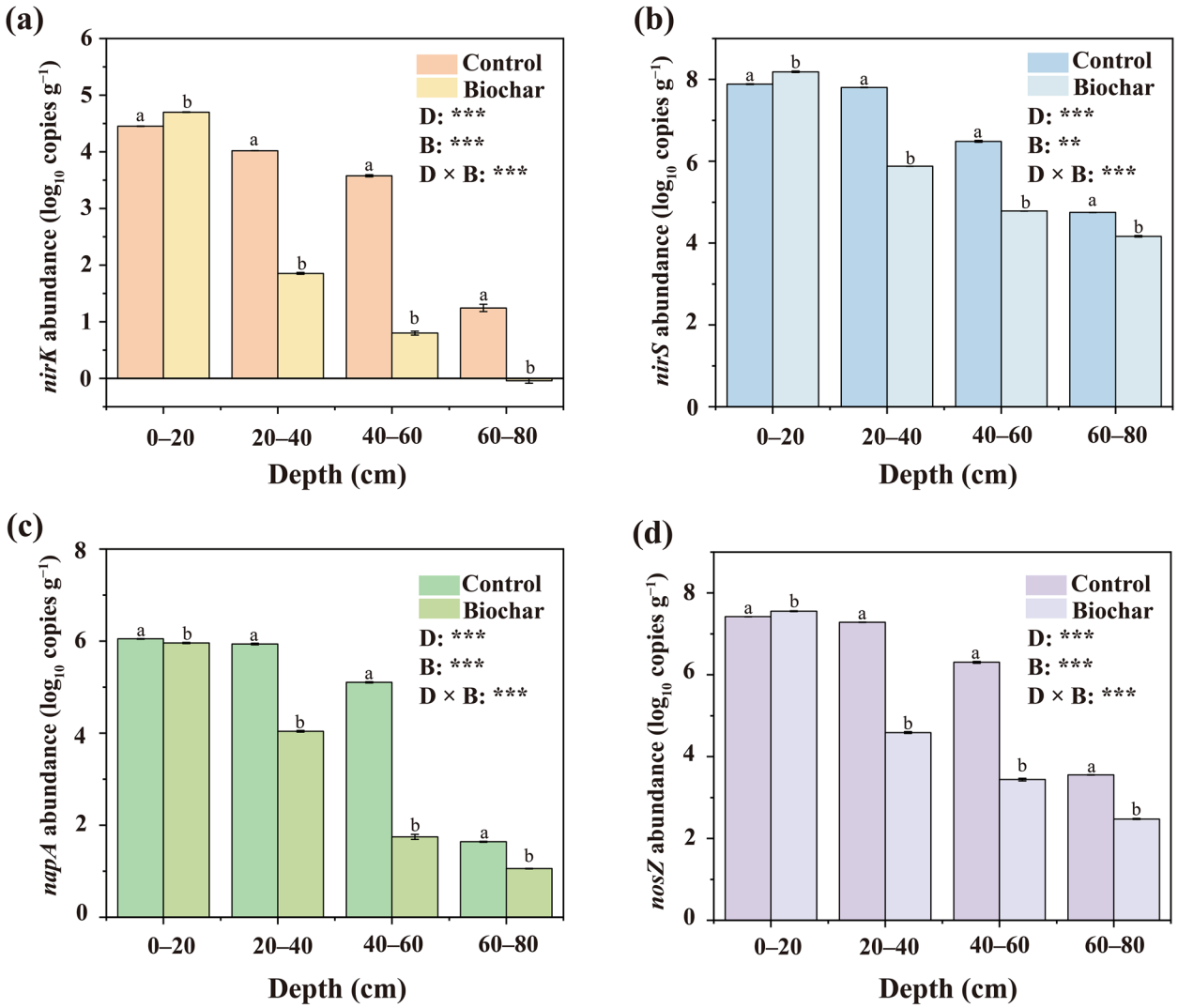

Fig. 2 Abundance (log_{10} copies g^{-1} dry soil) of nitrate reduction-related genes (*nirK*, *nirS*, *napA*, and *nosZ*) under control and biochar-amended paddy soil Error bars show the standard deviation of each treatment ($n = 3$). Different letters indicate significant differences at $P < 0.05$. The effects of sampling depth (D), biochar amendment (B), and their interaction (D × B) in each soil are shown. *$P < 0.05$; **$P < 0.01$; ***$P < 0.001$

reduced the abundance of all four functional genes in the 20–80 cm soil layer (Fig. 2), similar to the change of DNRA and denitrification rates in deep layers.

3.3 Diversity and composition of nitrate-reducing communities in biochar-amended paddy soil

For biochar amendment and depth combined effects, unconstrained principal coordinate analysis (PCoA) and permutation multivariate analysis of variance (PERMANOVA) showed significant differences in microbial community composition (i.e., encoding *nirK*, *nirS*, and *nosZ*) between BC and CK treatments ($P < 0.01$), with this divergence particularly pronounced along the first axis (Fig. 3a, c, e). The predominant *nirK* species were the Rhizobiales and unclassified_c_Alphaproteobacteria in the biochar treatments instead of the norank_d_Bacteria in CK treatment, which was consistent in all soil depths (Fig. 3b). The *nirS*-encoding species in CK and BC treatments group were norank_d_Bacteria and unclassified_p_Protecobacteria, respectively (Fig. 3d). The major *nosZ*-encoding species in the CK and BC treatments differed across soil depths (Fig. 3f). The primary species both in CK and BC treatments of 0–20 cm were Nitrosomonadales and unclassified Proteobacteria, but their relative proportions differed significantly. Nitrosomonadales decreased obviously and were replaced by Pseudomonadales, Rhizobiales, and unclassified_p_Protecobacteria in 20–40 cm soil. Compared to the CK

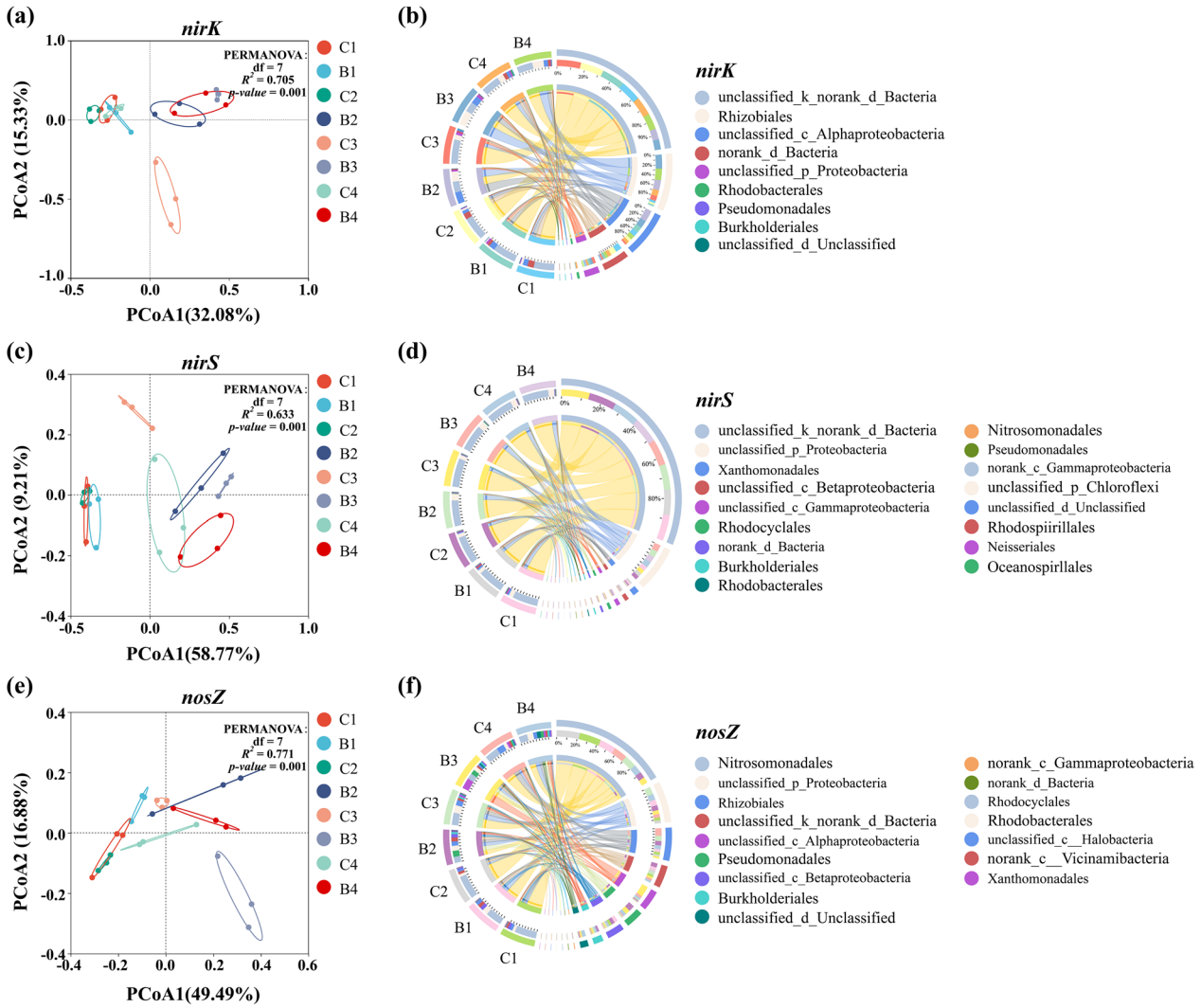

Fig. 3 Unconstrained principal coordinate analysis (PCoA) shows that soils from control and biochar-amended treatments at different depths have significantly distinct microbiota, as suggested by permutational multivariate analysis of variance (PERMANOVA): nitrate reducers encoded by the *nirS* (**a**), *nirK* (**c**), and *nosZ* (**e**) genes. Circos plots show the composition of *nirS* (**b**), *nirK* (**d**), and *nosZ* (**f**) encoding nitrate reducer communities at the order level in each treatment. The number on the inner ring and the length of the bars on the outer ring represent the relative abundance (percentage), respectively. C1: control of 0–20 cm; B1: biochar amendment of 0–20 cm; C2: control of 20–40 cm; B2: biochar amendment of 20–40 cm; C3: control of 40–60 cm; B3: biochar amendment of 40–60 cm; C4: control of 60–80 cm; B4: biochar amendment of 60–80 cm

treatment, Nitrosomonadales and Proteobacteria significantly decreased in BC treatment in the 40–60 cm layer, whereas the proportion of Alphaproteobacteria increased. BC treatment significantly reduced the proportions of Nitrosomonadales and Rhizobiales while increasing the proportion of Proteobacteria in 60–80 cm soil layer.

Our results further demonstrated that the denitrify genera had significant difference between CK and BC treatments, no matter in divided or all combined depths (Fig. S2). For *nirK*-encoding genera, norank_d_Bacteria abundance was significantly lower under BC treatment ($P < 0.01$) both in divided and combined layers (Fig. S2a). For *nirS*-encoding genera, *Paracoccus* and *Sulfuricella* abundances were markedly lower in BC treatment ($P < 0.01$), whereas *Azoarcus* abundance was significantly higher in BC treatment compared to CK treatment ($P < 0.05$) both in divided and combined layers (Fig. S2b). For *nosZ*-encoding genera, *Thiobacillus* and *Rhodoferax* abundances were significantly lower in BC treatment ($P < 0.01$, 0.05, respectively), whereas *Pseudomonas* abundance was significantly higher in BC treatment compared to CK treatment ($P < 0.05$) both in divided and combined layers (Fig. S2c).

3.4 Co-occurrence networks of denitrifying communities in biochar-amended paddy soil profiles

The interaction patterns across denitrifying (*nirK*, *nirS*, *nosZ*-encoding) bacteria in CK and BC treatments in different depths were explored through network analysis based on strong significant correlations (Fig. 4). The nodes and edges were merged between 0–20 cm and 20–40 cm. Similarly, the nodes and edges of 40–60 cm and 60–80 cm were merged because there were not enough samples to ensure the accuracy of the results. BC

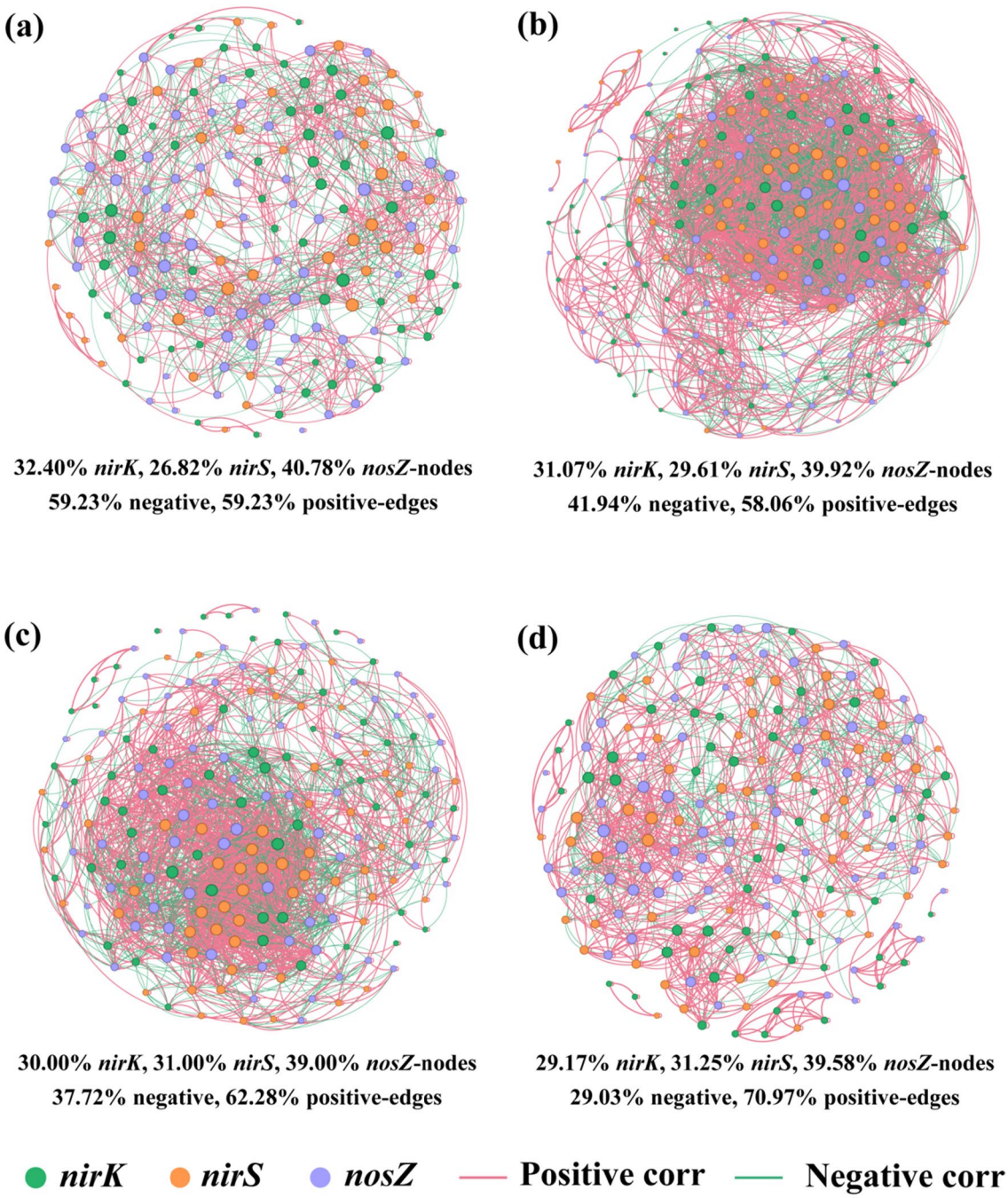

Fig. 4 Co-occurrence network analysis between *nirK*-, *nirS*-, and *nosZ*-encoding nitrate reducer communities (OTU level) in the Control and biochar treatments. 0–20 cm and 20–40 cm were combined of Control (**a**) and BC amendment (**b**), and 40–60 cm and 60–80 cm were combined of Control (**c**) and BC amendment (**d**), respectively

treatment exhibited fewer nodes but more edges than the control, resulting in higher network connectivity within the 0–40 cm soil layer (Fig. 4a, b). However, the trend was completely reversed for the 40–80 cm soil (Fig. 4c, d). By comparing the interactions and niches of different denitrifiers in each network, we found that they exhibited more interactions among *nirK*, *nirS*, and *nosZ*-encoding genera in BC treatment than CK treatment, characterized by increased positive correlations between them.

Keystone orders encoded by *nirS*, *nirK*, and *nosZ* genes in the 0–60 cm soil layer showed significant relationships with DNRA, denitrification, anammox rates, and relative contributions (%). For the 0–20 cm layer, the relationship between keystone orders and the three rates did not reveal significant competition among DNRA and denitrification and anammox, which was consistent with the rate change. Unclassified_c_Betaproteobacteria and unclassified_p_Proteobacteria were significantly positively correlated with denitrification, its contribution, and related genes. Norank _d_Bacteria and Thiobacillus showed opposite correlation (Fig. S3). For the 20–80 cm layer, the relationship between keystone orders and the three dissimilatory nitrate reduction rates showed significant competition, which was negatively correlated with DNRA rates whereas positively correlated with denitrification and anammox rates. The keystone orders included Thiobacillus, unclassified_o_Rhizobiales, and Rodoferax. The competition effect for all depths combined is also shown in Fig. S4. *Thiobacillus* showed a positive correlation with denitrification and anammox rates but a negative correlation with DNRA rates.

3.5 Key edaphic factors controlling denitrification, anammox, and DNRA across paddy soil profiles under biochar amendment

Mantel correlations were analyzed between DNRA, denitrification, and anammox rates, their respective proportions, and edaphic factors and microbial properties. For the 0–40 cm combined soil layer, anammox rate and its proportion showed significant positive correlations with functional gene (*napA*, *nirK*, *nirS*, *nosZ*) abundances and with edaphic factors (pH, SOC, NH_4^+–N, NO_3^-–N, SOC/NO_3^-, AP, Fe^{2+}) (Fig. 5a). Denitrification rates and their proportions showed significant positive correlations with functional gene (*napA*, *nirK*, *nirS*, *nosZ*) abundances and the edaphic factors (pH, SOC, NH_4^+–N, C/NO_3^-, SOC/NO_3^-, AP, Fe^{2+}) (Fig. 5a). DNRA rates and their proportions showed significant positive correlations with the abundances of functional genes (*napA*, *nirK*, *nirS*, *nosZ*) and with the edaphic factors (pH, SOC, NH_4^+–N, C/NO_3^-, SOC/NO_3^-, AP, Fe^{2+}) (Fig. 5a).

The correlation results in the combined 40–80 cm soil layer showed distinct differences from those in the 0–40 cm soil layer. Anammox rates and their proportions

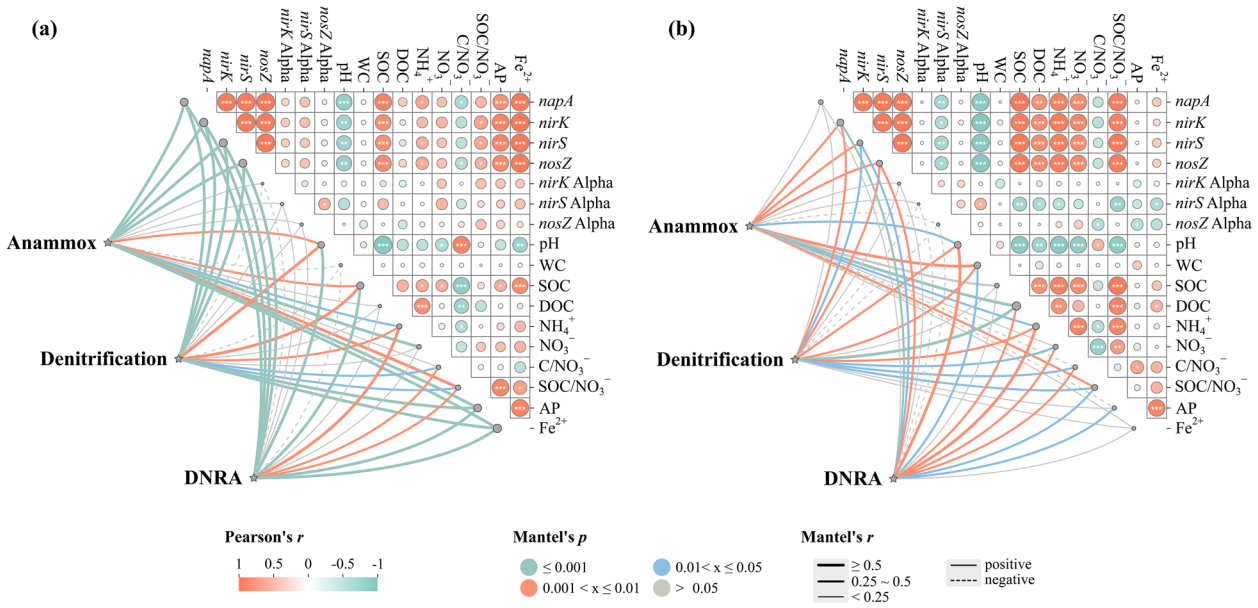

Fig. 5 Correlations between the associated gene abundances, alpha diversity of denitrification community, soil proprieties, and nitrate reduction rates (DNRA, denitrification, anammox rate, and relative contribution (%)) under control and biochar treatments in 0–40 cm (**a**) and 40–80 cm (**b**). The color gradient and square denote Pearson's correlation coefficients. Asterisks indicate statistical significance with levels of $^*P \le 0.05$, $^{**}P \le 0.01$, and $^{***}P \le 0.001$ for *P* values. Blue, orange, green, and gray edges indicate significant at $P < 0.05$, $P < 0.01$, $P < 0.001$ and non-significant relationships ($P \ge 0.05$), respectively. The alpha diversity of related microbes encoded by different genes is represented by the corresponding Shannon index.

showed significant positive correlations with functional gene (*nirK*, *nirS*, *nosZ*) abundances and with the edaphic factors (pH, water content: WC, DOC, NH_4^+–N, SOC/NO_3^-) (Fig. 5b). Denitrification rates and their proportions showed significant positive correlations with functional gene (*nirK*, *nirS*, *nosZ*) abundances and with edaphic factors (pH, WC, DOC, NH_4^+–N, NO_3^-–N, C/NO_3^-, SOC/NO_3^-) (Fig. 5b). DNRA rates and their proportions showed significant positive correlations with functional gene (*nirK*, *nirS*, *nosZ*) abundances and with the edaphic factors (pH, WC, DOC, NH_4^+–N, NO_3^-–N, C/NO_3^-, SOC/NO_3^-, AP) (Fig. 5b).

It is evident that dissimilatory nitrate reduction in different soil layers of paddy soil is primarily dominated by denitrification and DNRA. Therefore, random forest and structural equation modeling were employed to further elucidate the effects of depth and biochar amendment on soil denitrification and DNRA. The random forest results indicate that the abundance of *nirK* and *nosZ* functional genes and the edaphic variables of Fe^{2+}, SOC/NO_3^-, pH, and DOC are the primary factors influencing denitrification rates (Fig. 6a). The abundance of *napA* and *nirS* genes and the edaphic variables of pH, SOC/NO_3^-, NO_3^-, and TC are the primary factors influencing the denitrification/denitrification + DNRA ratio (Den/Den + DNRA) (Fig. 6c). Structural equation modeling further identified the primary microbial and edaphic variables influencing denitrification and DNRA processes under varying depths and biochar amendment. The datasets and structural equation models exhibited good fit, with the final models explaining over 90% of the variance in denitrification or DNRA rates (Fig. 6b, d). For the effect of biochar amendment, biochar amendment rate and Fe^{2+} content indirectly influenced soil denitrification rates by affecting *nosZ* gene abundance ($R^2 = 0.85$). Other edaphic factors such as DOC and pH directly impacted soil denitrification rates. Depth and pH indirectly influenced soil denitrification rates by affecting *nosZ* gene abundance ($R^2 = 0.86$). The edaphic factors of DOC and Fe^{2+} directly affected soil denitrification rates. The ratio of denitrification to DNRA, biochar amendment rate, and changes in SOC/NO_3^- indirectly influenced soil Den/Den + DNRA by affecting *napA* gene abundance ($R^2 = 0.95$). The factors of pH and Fe^{2+} directly influenced soil Den/Den + DNRA. Depth and pH indirectly influenced soil Den/Den + DNRA by affecting *napA* gene abundance ($R^2 = 0.86$). DOC and NO_3^- directly influenced Den/Den + DNRA.

4 Discussion

4.1 The role of denitrification and DNRA in regulating dissimilatory nitrate reduction in deep alkaline paddy soil under biochar amendment

Our results indicated that the rates of denitrification, DNRA, and anammox all significantly increased in the 0–20 cm soil layer. However, DNRA rate increased while denitrification and anammox rates decreased in the 20–40 cm layer (Fig. 1). These seemingly inconsistent effects are in fact reasonable. In the surface layer, biochar increased all the three rates, but denitrification showed the greatest increase (Fig. 1d). The primary reason is that the porous structure of biochar provides attachment sites for denitrifying bacteria (such as *Pseudomona*s and *Micrococcus*) and anaerobic ammonium-oxidizing bacteria (such as *Candidatus Brocadia*) (Zhou et al. 2016; Hafeez et al. 2022). On the other hand, biochar provides a large amount of readily degradable DOC, and the plow layer, influenced by rice root exudates (an additional carbon source), exhibits high carbon source availability (high C/N ratio), thereby satisfying the carbon requirements for both denitrification and DNRA (Pan et al. 2017; Pandey et al. 2020). Consequently, both denitrification and DNRA rates increased significantly. Compared to DNRA, denitrification has a competitive advantage under high C/N conditions, resulting in the greatest increase in its proportion (Li et al. 2022). At depths of 20–40 cm, readily degradable carbon sources such as DOC decrease, and pH changes are minimal; thus, carbon limitation becomes the primary limiting factor for the denitrification process (Ding et al. 2021). In contrast, DNRA rate continues to increase due to its low C/N requirements and pH adaptability (pH range 7.5–8.5), while denitrification is actually inhibited (Li et al. 2023; Kaviraj et al. 2024). Anammox process relies on nitrite as an electron acceptor. In deep paddy soils, the primary source of nitrite is an intermediate product of denitrification. Consequently, its trends mirror those denitrification processes. Furthermore, Fe^{2+} is more conducive to the DNRA process in alkaline paddy ecosystems, particularly in deeper soil layers.

Significant changes in soil denitrification rates and associated microbial communities are the primary factors driving depth-dependent variations in dissimilatory nitrate reduction under long-term biochar amendment. SEM results indicated that denitrification rates were influenced both by direct soil factors (DOC, pH, Fe^{2+}) and indirectly by related functional gene (*nosZ*) abundance (Figs. 5, 6a and b). Denitrification rates significantly decreased with increasing depth, primarily due to the following facts: (1) As soil depth increased, alkaline soil pH markedly rose, which inhibited *nosZ* gene abundance (Fig. 2d) and denitrifying microbial diversity (Figs. 5, 6b), particularly the abundance of *Thiobacillus* and *Rodoferax*

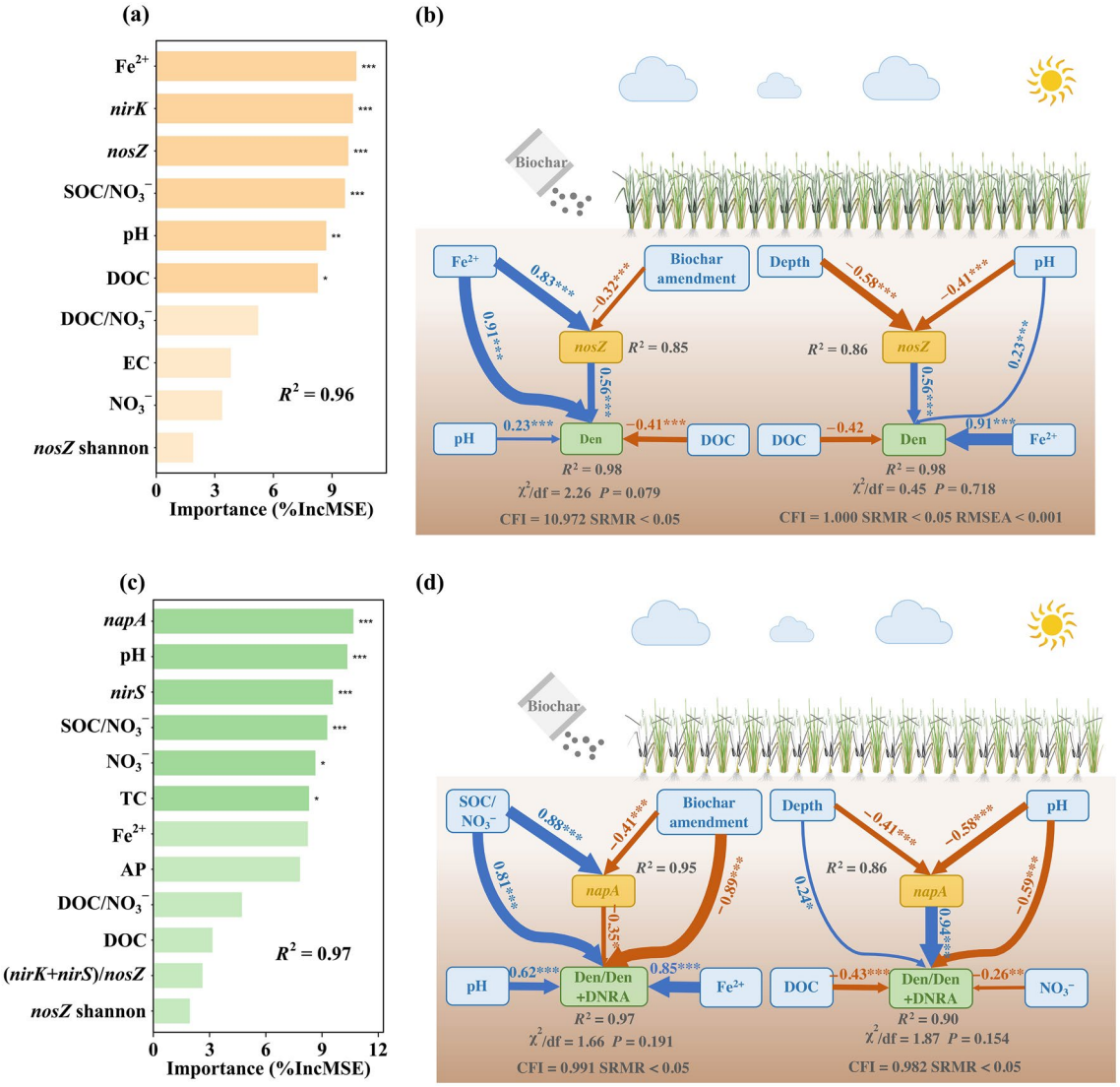

Fig. 6 Importance of predictors for denitrification rate (**a**) and Denitrification/ Denitrification + DNRA (Den/Den + DNRA) ratio (**c**) in paddy soils based on the random forest analyses. Structural equation model based on effects of abiotic and biotic environmental factors on the denitrification rate (**b**) and Den/Den + DNRA ratio (**d**). Blue and orange solid arrows indicate significant positive and negative relationships, respectively. The thickness of the arrows is directly proportional to the standardized path coefficient on the single arrow. R^2 represents the variance of factors explained by the model

(Figs. 3, S2 and S3), thereby suppressing soil denitrification rates; (2) Similarly, DOC concentrations also significantly decreased with increasing soil depth (Table 1). On the one hand, substrate availability for heterotrophic denitrifying bacteria remained constrained (Qin et al. 2019). On the other hand, DOC, acting as an electron donor, significantly decreased (Ding et al. 2021), leading to a sharp decline in *nosZ* abundance (Fig. 2) and microbial diversity (especially *Thiobacillus* and *Rodoferax*), which in turn suppressed denitrification rates (Figs. S2, S3); (3) There was a decreased Fe^{2+} concentration. Fe^{2+} in deep soil may oxidize to Fe^{3+}, thereby weakening its role of electron-transfer function and further inhibiting denitrification (Cayuela et al. 2013, 2014). Biochar amendment amplified the decline in denitrification rates associated with increased depth (Fig. 1b). Biochar further increased soil pH and reduced DOC concentration, both of which persistently suppressed *nosZ* gene expression (Fig. 2d) and related *nosZ*-encoding genera (*Thiobacillus* and *Rodoferax*) (Fig. S2). In general, the optimal pH for *nosZ* enzyme activity is near neutral, with significant inhibition occurring above pH 8 or 8.5 (Frostegård et al.

2022). Soil pH reached a maximum of 8.10, leading to a more pronounced decrease in denitrification rates under long-term biochar amendment.

Our results indicated that DNRA also plays a vital role in regulating dissimilatory nitrate reduction under long-term biochar amendment. DNRA rates decreased with increasing depth, most markedly between 60 and 80 cm, though less markedly than denitrification rates (Fig. 1a). However, qPCR analysis failed to detect the abundance of the *nrfA* functional gene (its abundance $< 10^3$ copies g^{-1}). This is probably because the observed DNRA rate is primarily driven by non-biochemical nitrate reduction, which is not related to the *nrfA*-encoding microbial community. The specific reasons are as follows: (1) although the alkaline environment in the studied paddy soil is suitable for *nrfA*-encoding microbial communities (with an optimal pH of 7.5–8.5), SOC and DOC concentrations drop sharply in deep soil, causing *nrfA* bacteria to decline sharply due to their inability to obtain sufficient energy (Wei et al. 2023); (2) high NO_3^- concentration combined with reduced SOC and DOC in alkaline paddy soils leads to a significant decrease in the ratio of SOC/NO_3^- and DOC/NO_3^- (Table 1), thereby inhibiting *nrfA* gene expression; (3) alkaline paddy soils (particularly in the coastal areas of Tianjin) are often rich in Fe^{2+}. Under deep anaerobic conditions, NO_2^- can be chemically reduced directly to NH_4^+ through Fe^{2+}, which not require *nrfA*-encoding enzyme (Robertson and Thamdrup 2017; Pandey et al. 2020). Therefore, the fact that *nrfA* gene was not detected in our alkaline paddy soils does not affect the analysis of controlling factors of DNRA process.

Our results indicated that changes in DNRA process were regulated by soil pH, SOC/NO_3^-, and AP (Fig. 5). With increasing depth, soil pH significantly increased, while SOC/NO_3^- and AP significantly decreased (Table 1). The decline in SOC/NO_3^- and AP directly led to a decline of soil DNRA rates, as both parameters showed significant positive correlations with DNRA (Fig. 5). SOC/NO_3^- has been widely shown to have a significant positive relationship with DNRA rates (Zhang et al. 2021; Wei et al. 2022), because fermentable C (such as glucose and glycerol) serves as an electron donor source and NO_3^- as an electron acceptor (Zhou et al. 2016; Pandey et al. 2020). In addition, decreased AP significantly reduced soil organic matter decomposition activity, leading to decreased electron donors (Yuan et al. 2022) and consequently inhibiting the DNRA process. Although soil pH continued to increase with soil depth, values approaching or exceeding eight slightly inhibited DNRA-related enzyme activities, resulting in a marginal decrease in DNRA rates. Long-term biochar amendment mitigated the decline in DNRA rates induced by increased soil depth, though it showed a downward trend (Fig. 1a). The primary reason is that biochar amendment increased soil AP content (Table 1), which is consistent with previous findings (Joseph et al. 2021). The increase in AP mitigated the decline in DNRA rates. This is mainly due to (1) an increase in AP content can alleviate microbial phosphorus limitation in deep soil, promoting the growth and maintenance of the functional microbial community involved in DNRA, thereby partially offsetting the decline in DNRA rates caused by reduced DOC and anaerobic conditions; (2) increased soil AP can enhance the α-diversity of DNRA microbial community, as well as its energy metabolism and the activity of related enzymes, enabling it to continue performing DNRA even under low-carbon conditions (Wang et al. 2022); (3) higher AP content promotes the dominant DNRA microbial community, providing a competitive advantage over denitrifying bacteria (Huang et al. 2025). Even though DOC decreases with depth, a simultaneous increase in AP can provide a certain "protective effect" for soil DNRA process, thereby reducing its decline to some extent. In summary, long-term biochar amendment significantly suppressed denitrification rates in deep alkaline paddy soils while relatively promoting DNRA processes, thereby enhancing deep soil N retention.

4.2 Mechanisms associated with the trade-off between denitrification and DNRA in alkaline deep paddy soil under biochar amendment

Long-term biochar amendment had significantly different impacts on denitrification and DNRA processes across different soil layers. In the topsoil, biochar amendment simultaneously enhanced the absolute rates of denitrification and DNRA, while denitrification accounted for a significantly higher proportion than DNRA (Fig. 1d). The simultaneous increase in denitrification and DNRA were primarily attributed to soil pH rising from 6.8 to 7.4 due to biochar amendment, which favors the transcriptional activity of *nirK* and *nrfA* (Kajie and Anraku 1986). Moreover, *nirK* exhibits optimal activity at pH < 7.0, while *nrfA* activity peaks at pH > 7.5 (Kim et al. 2017), leading to a greater increase in denitrification compared to DNRA rates. Secondly, biochar significantly increased soil SOC/NO_3^- and DOC/NO_3^- ratios (Table 1), with SOC/NO_3^- exerting a significant positive effect on Den/Den + DNRA ratio (Fig. 6d). This was mainly because increased concentrations of SOC and DOC, acting as electron donors, simultaneously promoted denitrification and DNRA (Li et al. 2020a; Zhang et al. 2021). Thirdly, Fe^{2+} concentration also significantly increased under long-term biochar amendment (Table 1), which is consistent with previous findings (Joseph et al. 2021). Direct evidence showed that there was a significant positive correlation between Fe^{2+} concentration and denitrification and DNRA rates

(Fig. 5a), primarily because Fe^{2+} acted as an electron donor for both processes. Higher Fe^{2+} concentrations directly increased both denitrification and DNRA rates (Pandey et al. 2020). DNRA process generally transferred more electrons (8 e^-) than denitrification process (5 e^-) (van den Berg et al. 2015), and thus, denitrification was promoted more significantly than DNRA. Overall, long-term biochar amendment primarily regulated the relative proportions of denitrification and DNRA by influencing soil pH and Fe^{2+} concentration in the surface soil layer.

Soil denitrification rate significantly decreased while the DNRA rate markedly increased with increasing soil depth (Fig. 1d). Long-term biochar amendment significantly decreased the denitrification proportion while it increased the DNRA proportion, which was opposite to that observed in the surface layer. Furthermore, the Den/Den + DNRA ratio showed more decrease with increasing depth (Fig. 1d). Concentrations of SOC, DOC, and NO_3^- significantly decreased, and SOC and DOC showed greater decrease than NO_3^-. The primary reasons for the gradual decrease in SOC and DOC concentration with increasing soil depth are that: (1) the root biomass decreases sharply as soil depths increase, resulting in minimal DOC input to deeper soil layers (Aumtong et al. 2023); and (2) as depth increases, microbial diversity and activity decline due to anaerobic conditions, leading to a slower rate of organic matter decomposition and a reduction in DOC production, which was particularly pronounced under alkaline conditions (He et al. 2015). This effect was particularly pronounced under long-term biochar amendment, leading to more decrease in SOC/NO_3^- and DOC/NO_3^- ratios (Table 1). This is attributed to the continuous microbial consumption of labile C during migration to soil deep layers, allowing only recalcitrant C (e.g., aromatic compounds) to leach to deeper soil layers for microbial utilization, while NO_3^- was consumed only in anaerobic zones (Yoon et al. 2015; Pandey et al. 2020). Characterized by its large specific surface area and porous structure, biochar can adsorb free organic carbon and significantly reduce the DOC concentration in soil (Lehmann et al. 2011). In addition, it provides habitats for microorganisms and promotes the immobilization of DOC into microbial biomass, which constitutes the primary cause for the reduction of soil DOC. Under alkaline conditions, soil organic matter tends to form negatively charged colloids (Yuan et al. 2017). Since the surface of biochar is also negatively charged, electrostatic repulsion inhibits the direct attachment of DOC to biochar, which in turn expands the physical interception capacity of biochar porosity and leads to a significant decline in DOC content (Wu et al. 2021; Zhang et al. 2023). Denitrification is highly dependent on carbon sources, and a sharp reduction in C sources significantly suppressed the denitrification process. Conversely, the DNRA pathway showed greater advantage in anaerobic zones (Lu et al. 2013). With pH exceeding 8 in deep soil layers (Table 1), *nrfA* protein expression becomes feasible (Bai et al. 2020), while denitrification-related proteins are in turn suppressed. Furthermore, although Fe^{2+} concentration decreased with soil depth, biochar amendment and diffusion mitigated this decline in Fe^{2+} concentration (Table 1). The depletion of electron donor Fe^{2+} and electron acceptor NO_3^- with increased depth was mitigated due to biochar amendment. Thus, DNRA process showed a competitive advantage over denitrification process when both electron donors and acceptors were relatively abundant (Kraft et al. 2014; Zhao et al. 2021). Thus, soil pH, C availability, and Fe^{2+} concentration are key factors influencing the competitive dynamics between denitrification and DNRA processes in deep alkaline paddy soils.

4.3 Depth-dependent suppression of anammox under biochar amendment

Soil anammox process, acting as a main N loss pathway, was also strongly influenced by the combined effect of depth and biochar amendment (Gu et al. 2017). While denitrification and DNRA processes dominated total dissimilatory nitrate reduction, anammox had measurable contributions in surface layers (23.47% in 0–20 cm) that declined dramatically with depth to only 1.85% in the 60–80 cm soil layer (Fig. 1d). Biochar significantly suppressed the proportion of anammox rates across all soil layers, with the most pronounced effects in deep layers where rates decreased from 10.8% to 1.90% in the 60–80 cm layer. This suppression likely results from multiple interacting factors. First, anammox bacteria are highly sensitive to pH, with optimal activity between pH 7.0 and 8.5 and significant inhibition above pH 8.5 (Shan et al. 2018; Yang et al. 2025a). The pH increase to 8.10–8.12 in deep biochar-amended layers approached or exceeded this inhibitory threshold. Second, anammox bacteria require both NH_4^+ and NO_2^- as substrates. In deep layers, NO_2^- availability likely became limiting as denitrification was suppressed and DNRA consumed available nitrate, converting it to NH_4^+ rather than producing NO_2^- intermediates (Wei et al. 2022). This was confirmed by the opposite trend between anammox and DNRA across soil depth (Fig. 1). Third, anammox bacteria abundance typically increases with depth in paddy soils where O_2 concentrations are lower, but our results suggested that in alkaline systems, pH constraints likely override the favorable O_2 conditions.

The near-complete suppression of anammox in deep alkaline layers under biochar amendment has important implications. Since anammox contributes to N loss from

the system, its very low rates in these conditions mean that the N retention benefits of enhanced DNRA are not substantially offset by anammox activity. This contrasts with neutral to slightly acidic paddy soils where anammox can account for 4.5–37% of N loss (Xi et al. 2016), highlighting the unique N cycling dynamics in alkaline deep paddy soils. Soil pH markedly increased under long-term BC treatment (pH > 8, Table 1), which significantly inhibited anammox. Soil Fe^{2+} content markedly decreased along the profile, even with a slight increase under BC treatment (Table 1). Low Fe^{2+} concentrations significantly suppressed anammox rates (Huang et al. 2014; Li et al. 2020a). This contrasts sharply with the results for anammox in deep, non-alkaline soils regarding soil N loss (Ding et al. 2021). In summary, the vital role of anammox processes in causing N loss in alkaline deep paddy soils was overestimated, particularly under long-term biochar amendment.

4.4 Implications for dissimilatory nitrate reduction in paddy soil profile

Compared to previous studies focused on acidic paddy soils, this research fills a gap in understanding the effects of long-term biochar amendment on dissimilatory reduction processes in alkaline paddy soil. This study demonstrated that long-term biochar amendment simultaneously increased denitrification and DNRA rates while increasing the Den/Den + DNRA ratio. Conversely, long-term biochar amendment increased DNRA/Den + DNRA ratio in acidic soils (Wei et al. 2022). A meta-analysis also confirmed that biochar amendment promoted DNRA processes in acidic soils (Yang et al. 2025b). Although biochar increases denitrification in the surface layer of the alkaline paddy soil, the deeper soil in turn showed a higher proportion of DNRA (Fig. 1). The results indicated that long-term biochar amendment favors DNRA processes in deeper soil layers, thereby reducing soil N loss. Alkaline paddy soils are widely distributed in arid-semiarid irrigated agricultural regions. Long-term application of biochar can effectively sequester available N from DNRA in deep soils, thereby enhancing plant N uptake and ultimately boosting crop yield.

Biochar aging significantly alters its specific surface area, pore volume, pH, elemental content, and migration (Wang et al. 2020). First, as natural aging progresses, the specific surface area and pore volume of biochar may either increase or decrease. This is typically closely linked to biochar oxidation, mineral dissolution, and DOM release, which significantly alter microbial colonization and reactions in denitrification and DNRA. Second, biochar aging can reduce its ash content and pH value (Ren et al. 2018). In addition, biochar aging enhances the migration of biochar particles, which may explain why DNRA processes are not inhibited by strong alkalinity as soil depth increases. On the other hand, labile C significantly decreases in aging biochar, while the remaining recalcitrant C cannot be utilized by most denitrifying microorganisms, leading to weakened denitrification (He et al. 2019). Therefore, changes in soil C fractions caused by biochar aging significantly altered the interactions between denitrification and DNRA processes. The lack of understanding of how the variations of different C fractions due to biochar aging affecting soil nitrate dissimilatory reduction processes is also a limitation of this study. Future research is needed to compare the effects of fresh biochar and naturally aged biochar on soil nitrate dissimilatory reduction processes.

Our study demonstrated that five years of biochar amendment increased DNRA rates while suppressing denitrification and anammox rates with increasing soil depth, highlighting the role of biochar in regulating dissimilatory nitrate reduction and N cycling in alkaline deep paddy soils. Although the effects of biochar amendment on soil denitrification (Zhang et al. 2024), anammox (Yang et al. 2025a), and DNRA (Yang et al. 2025b) processes have been reported at a global scale, the dynamics of these processes remain unclear and need further research. This is because we can reveal the competition and interactions between denitrification and DNRA only by simultaneously quantifying the dynamics of three processes and related microbial community, thereby avoiding overestimating or underestimating the impact of any single process on soil N flux. For example, high pH may inhibit denitrifying microbes but potentially promote anammox-related microbes in alkaline paddy soil. Focusing solely on denitrification could lead to an inaccurate assessment of soil total N loss. Based on our findings, we infer that biochar likely reduced soil nitrogen (N) losses. The significant reduction in N loss via denitrification and anammox (20–80 cm, Fig. 1) and the enhanced DNRA likely had a greater impact on overall N loss under biochar amendment (Zhang et al. 2021). This is because N transformation processes in the deep soil directly determine whether nitrate leaches into groundwater or is further converted into gaseous losses, and the reduction in deep denitrification and anammox directly reduces these losses under biochar amendment (Pandey et al. 2019; Ding et al. 2021). Therefore, future research should consider the dynamics of three processes under different cropland management and monitoring of N_2O gas losses and N leaching to provide a theoretical basis for accurately assessing soil N cycling in agroecosystems.

5 Conclusion

This study investigated the partitioning of nitrate reduction pathways in an alkaline deep paddy soil following five years of biochar amendment. Across the soil profile, denitrification rates declined sharply with depth, whereas DNRA rates became progressively more dominant with depths. Biochar amendment increased the absolute rates of denitrification, anammox, and DNRA in the surface layer of alkaline paddy soil, yet altered their relative importance: biochar amendment enhanced denitrification in surface soil, while in deep layers it suppressed denitrification and anammox but promoted DNRA. Structural equation modeling and random forest analysis showed that these shifts were governed primarily by changes in the edaphic variables of soil pH, DOC, SOC/NO_3^- ratio, and Fe^{2+} concentration, acting through their effects on *nosZ* and *napA* gene abundances. In deep layers, increased pH (>8.0), lower DOC availability, and reduced Fe^{2+} concentrations decreased *nosZ* and *napA* abundances, thereby constraining denitrification but favoring DNRA. Collectively, these findings demonstrate that long-term biochar amendment in alkaline paddy soil enhances N retention by steering nitrate reduction away from gaseous loss pathways (denitrification and anammox) toward DNRA in deep layers, while stimulating denitrification in the surface layer. This depth-dependent re-partitioning of nitrate reduction provides mechanistic evidence that biochar probably can be an effective tool for conserving N in alkaline paddy systems, but also highlights the need to consider soil depth and initial pH when designing biochar-based N management strategies.

Supplementary Information

The online version contains supplementary material available at https://doi.org/10.1007/s42773-026-00645-5.

Supplementary Material 1.

Author contributions

Qiannan Yang: Conceptualization, Data curation, Formal analysis, Investigation, Methodology, Software, Validation, Visualization, Writing original draft, Writing—review & editing. Guilong Zhang: Conceptualization, Funding acquisition, Validation, Writing—review and editing. Jie Li: Conceptualization, Data curation, Investigation, Methodology, Supervision, Project administration. Hu Li: Supervision, Validation, Writing—review & editing. Lukas Van Zwieten: Validation, Supervision, Writing–review & editing. Lili Wang: Conceptualization, Supervision, Writing–review & editing. All authors read and approved the final manuscript.

Funding

This work was supported by the Innovation Program of Chinese Academy of Agricultural Sciences (CAAS-CSGLCA-202402), the China Postdoctoral Science Foundation (2024M761540), National Natural Science Foundation of China (32573156), and the China Postdoctoral Science Foundation-Tianjin Joint Support Program (2023T007TJ).

Data availability

The datasets used or analyzed in this study are available from the corresponding author upon reasonable request.

Declarations

Competing interests

Lukas Van Zwieten is an EBM of the journal Biochar, and he was not involved in the peer-review or handling of the manuscript. The authors declare no conflicts of interest.

Author details

[1]Agro-Environmental Protection Institute, Ministry of Agriculture and Rural Affairs, Tianjin, China. [2]Qingyun Field Comprehensive Scientific Observation and Research Station of the Ministry of Agriculture and Rural Affairs, Qingyuan, China. [3]Modern Agricultural Science and Technology Experimental Demonstration Base for Crop Cultivation and Resource Environment of the Ministry of Agriculture and Rural Affairs (Qingyun), Qingyuan, China. [4]State Key Laboratory of Efficient Utilization of Arable Land in China, Institute of Agricultural Resources and Regional Planning, Chinese Academy of Agricultural Sciences, Beijing, China. [5]NSW Department of Primary Industries, Wollongbar Primary Industries Institute, Wollongbar, NSW, Australia.

Received: 6 April 2026 Revised: 4 June 2026 Accepted: 25 June 2026
Published online: 08 September 2026

References

Aumtong S, Chotamonsak C, Pongwongkam P, Cantiya K (2023) Chemical fertilization alters soil carbon in paddy soil through the interaction of labile organic carbon and phosphorus fractions. Agronomy 13:1588. https://doi.org/10.3390/agronomy13061588

Bai R, Fang Y, Mo L, Shen J, Song L, Wang Y, Zhang L, He J (2020) Greater promotion of DNRA rates and *nrfA* gene transcriptional activity by straw incorporation in alkaline than in acidic paddy soils. Soil Ecol Lett 2(4):255–267. https://doi.org/10.1007/s42832-020-0050-6

Bao S (2000) Chemical analysis for agricultural soil. China Agriculture Press, Beijing, China

van den Berg EM, van Dongen U, Abbas B, van Loosdrecht CM (2015) Enrichment of DNRA bacteria in a continuous culture. The ISME J 9:2153–2161. https://doi.org/10.1038/ismej.2015.26

Caporaso JG, Kuczynski J, Stombaugh J, Bittinger K, Bushman FD, Costello EK, Fierer N, Pena AG, Goodrich JK, Gordon JI (2010) QIIME allows analysis of high-throughput community sequencing data. Nat Methods 7:335–336. https://doi.org/10.1038/nmeth.f.303

Cayuela ML, Sánchez-Monedero MA, Roig A, Hanley K, Enders A, Lehmann J (2013) Biochar and denitrification in soils: when, how much and why does biochar reduce N_2O emissions? Sci Rep 3:1732. https://doi.org/10.1038/srep01732

Cayuela ML, van Zwieten L, Singh BP, Jeffery S, Roig A, Sánchez-Monedero MA (2014) Biochar's role in mitigating soil nitrous oxide emissions: a review and meta-analysis. Agr Ecosyst Environ 191:5–16. https://doi.org/10.1016/j.agee.2013.10.009

Cheng Y, Elrys AS, Merwad A-RM, Zhang H, Chen Z, Zhang J, Cai Z, Müller C (2022) Global patterns and drivers of soil dissimilatory nitrate reduction to ammonium. Environ Sci Technol 56(6):3791–3800. https://doi.org/10.1021/acs.est.1c07997

Csárdi G, Nepusz T (2006) The igraph software package for complex network research. J Sci Comput 1695:1–9

Ding B, Zhang H, Luo W, Sun S, Cheng F, Li Z (2021) Nitrogen loss through denitrification, anammox and Feammox in a paddy soil. Sci Total Environ 773:145601. https://doi.org/10.1016/j.scitotenv.2021.145601

Edgar RC (2010) Search and clustering orders of magnitude faster than BLAST. Bioinformatics 26(19):2460–2461. https://doi.org/10.1093/bioinformatics/btq461

Frostegård Å, Vick SHW, Lim NYN, Bakken LR, Shapleigh JP (2022) Linking meta-omics to the kinetics of denitrification intermediates reveals pH-dependent causes of N_2O emissions and nitrite accumulation in soil. ISME J 16(1):26–37. https://doi.org/10.1038/s41396-021-01045-2

Gao D, Tian H, Yang H, Tan W, Liang X, Wen C, Song D, Zhang Y, Tan Q (2025) Co-application of digestate and biochar reduced greenhouse gas emissions in paddy soil through enhanced denitrification and anaerobic methane oxidation. J Environ Manage 381:125244. https://doi.org/10.1016/j.jenvman.2025.125244

Gu C, Zhou H, Zhang Q, Zhao Y, Di H, Liang Y (2017) Effects of various fertilization regimes on abundance and activity of anaerobic ammonium oxidation bacteria in rice-wheat cropping systems in China. Sci Total Environ 599–600:1064–1072. https://doi.org/10.1016/j.scitotenv.2017.04.240

Hafeez A, Pan T, Tian J, Cai K (2022) Modified biochars and their effects on soil quality: a review. Environments 9(5):60. https://doi.org/10.3390/environments9050060

He Y, Siemens J, Amelung W, Goldbach H, Wassmann R, Alberto MCR, Lücke A, Lehndorff E (2015) Carbon release from rice roots under paddy rice and maize–paddy rice cropping. Agr Ecosyst Environ 210:15–24. https://doi.org/10.1016/j.agee.2015.04.029

He L, Shan J, Zhao X, Wang S, Yan X (2019) Variable responses of nitrification and denitrification in a paddy soil to long-term biochar amendment and short-term biochar addition. Chemosphere 234:558–567. https://doi.org/10.1016/j.chemosphere.2019.06.038

Hou L, Liu M, Carini SA, Gardner WS (2012) Transformation and fate of nitrate near the sediment-water interface of Copano Bay. Cont Shelf Res 35:86–94. https://doi.org/10.1016/j.csr.2012.01.004

Huang X, Gao D, Peng S, Tao Y (2014) Effects of ferrous and manganese ions on anammox process in sequencing batch biofilm reactors. Environ Sci 26:1034–1039. https://doi.org/10.1016/S1001-0742(13)60531-8

Huang J, Tie W, Jiang D, Huang X (2025) Dissimilatory nitrate reduction to ammonium bacterial communities differences in lateritic red soil depends on soil properties. J Soil Sediment 25:3984–4001. https://doi.org/10.1007/s11368-025-04165-w

Jia M, Winkler MKH, Volcke EIP (2020) Elucidating the competition between heterotrophic denitrification and DNRA using the resource-ratio theory. Environ Sci Technol 54(21):13953–13962. https://doi.org/10.1021/acs.est.0c01776

Joseph S, Husson O, Graber ER, Van Zwieten L, Taherymoosavi S, Thomas T, Nielsen S, Ye J, Pan G, Chia C (2015) The electrochemical properties of biochars and how they affect soil redox properties and processes. Agronomy 5(3):322–340. https://doi.org/10.3390/agronomy5030322

Joseph S, Cowie AL, Van Zwieten L, Bolan N, Budai A, Buss W, Cayuela ML, Graber ER, Ippolito JA, Kuzyakov Y, Luo Y, Sik Ok Y, Palansooriya KN, Shepherd J, Stephens S, Weng Z, Lehmann J (2021) How biochar works, and when it doesn't: a review of mechanisms controlling soil and plant responses to biochar. Glob Change Biol Bioenergy 13:1731–1764. https://doi.org/10.1111/gcbb.12885

Kajie S, Anraku Y (1986) Purification of a hexaheme cytochrome C552 from Escherichia coli K12 and its properties as a nitrite reductase. Eur J Biochem 154:457–463. https://doi.org/10.1111/j.1432-1033.1986.tb09419.x

Kaviraj M, Kumar U, Chatterjee S, Parija S, Padbhushan R, Nayak AK, Gupta VVSR (2024) Dissimilatory nitrate reduction to ammonium (DNRA): a unique biogeochemical cycle to improve nitrogen (N) use efficiency and reduce N-loss in rice paddy. Rhizosphere 30:100875. https://doi.org/10.1016/j.rhisph.2024.100875

Kim H, Park D, Yoon S (2017) pH control enables simultaneous enhancement of nitrogen retention and N_2O reduction in Shewanella loihica strain PV-4. Front Microbiol 8:1820. https://doi.org/10.3389/fmicb.2017.01820

Kraft B, Tegetmeyer HE, Sharma R, Klotz MG, Ferdelman TG, Hettich RL, Geelhoed JS, Strous M (2014) The environmental controls that govern the end product of bacterial nitrate respiration. Science 348(80):676–679. https://doi.org/10.1126/science.1252215

Lehmann J, Rillig MC, Thies J, Masiello CA, Hockaday WC, Crowley D (2011) Biochar effects on soil biota e A review. Soil Biol Biochem 43:1812–1836. https://doi.org/10.1016/j.soilbio.2011.04.022

Li X, Sardans J, Gargallo-Garriga A, Asensio D, Vallicrosa H, Peñuelas J (2020a) Nitrogen reduction processes in paddy soils across climatic gradients: key controlling factors and environmental implications. Geoderma 368:114275. https://doi.org/10.1016/j.geoderma.2020.114275

Li X, Song C, Zhou Z, Xiao J, Wang S, Yang L, Cao X, Zhou Y (2020b) Comparison of community and function of dissimilatory nitrate reduction to ammonium (DNRA) bacteria in Chinese shallow lakes with different eutrophication degree. Water 12:174. https://doi.org/10.3390/w12010174

Li X, Wang G, Chen J, Zhou X, Liu Y (2022) Deciphering the concurrence of comammox, partial denitrification and anammox in a single low-oxygen mainstream nitrogen removal reactor. Chemosphere 305:135409. https://doi.org/10.1016/j.chemosphere.2022.135409

Li C, Wei Z, Wang X, Ma X, Yang P, Shan J, Yan X (2023) Long-term fertilization regulates dissimilatory nitrate reduction processes by altering paddy soil organic carbon components. Soil Use Manage 00:1–14. https://doi.org/10.1111/sum.12994

Liu C, Hou L, Liu M, Zheng Y, Yin G, Han P, Dong H, Gao J, Gao D, Chang Y, Zhang Z (2019) Coupling of denitrification and anaerobic ammonium oxidation with nitrification in sediments of the Yangtze Estuary: importance and controlling factors. Estuar Coast Shelf S 220:64–72. https://doi.org/10.1016/j.ecss.2019.02.043

Lu W, Zhang H, Shi W (2013) Dissimilatory nitrate reduction to ammonium in an anaerobic agricultural soil as affected by glucose and free sulfide. Eur J Soil Biol 58:98–104. https://doi.org/10.1016/j.ejsobi.2013.07.003

Mctigue ND, Gardner WS, Dunton KH, Hardison AK (2016) Biotic and abiotic controls on co-occurring nitrogen cycling processes in shallow Arctic shelf sediments. Nat Commun 7:13145. https://doi.org/10.1038/ncomms13145

Pan F, Chapman SJ, Li Y, Yao H (2017) Straw amendment to paddy soil stimulates denitrification but biochar amendment promotes anaerobic ammonia oxidation. J Soils Sediments 17:2428–2437. https://doi.org/10.1007/s11368-017-1694-4

Pandey A, Suter H, He J, Hu H, Chen D (2019) Dissimilatory nitrate reduction to ammonium dominates nitrate retention in long-term low nitrogen fertilized rice paddies. Soil Biol Biochem 131:149–156. https://doi.org/10.1007/s00374-020-01508-2

Pandey CB, Kumar U, Kaviraj M, Minick KJ, Mishra AK, Singh JS (2020) DNRA: a short-circuit in biological N-cycling to conserve nitrogen in terrestrial ecosystems. Sci Total Environ 738:139710. https://doi.org/10.1016/j.scitotenv.2020.139710

Qin H, Xing X, Tang Y, Zhu B, Wei X, Chen X, Liu Y (2019) Soil moisture and activity of nitrite- and nitrous oxide-reducing microbes enhanced nitrous oxide emissions in fallow paddy soils. Biol Fertil Soils 56:53–67. https://doi.org/10.1007/s00374-019-01403-5

Ren X, Sun H, Wang F, Zhang P, Zhu H (2018) Effect of aging in field soil on biochar's properties and its sorption capacity. Environ Pollut 242:1880–1886. https://doi.org/10.1016/j.envpol.2018.07.078

Robertson EK, Thamdrup B (2017) The fate of nitrogen is linked to iron (II) availability in a freshwater lake sediment. Geochim Cosmochim Act 205:84–99. https://doi.org/10.1016/10.1016/j.gca.2017.02.014

Shan J, Zhao X, Sheng R, Xia Y, Ti C, Quan X, Wang S, Wei W, Yan X (2016) Dissimilatory nitrate reduction processes in typical Chinese paddy soils: rates, relative contributions, and influencing factors. Environ Sci Technol 50:9972–9980. https://doi.org/10.1021/acs.est.6b01765

Shan J, Yang P, Shang X, Rahman MM, Yan X (2018) Anaerobic ammonium oxidation and denitrification in a paddy soil as affected by temperature, pH, organic carbon, and substrates. Biol Fert Soils 54(3):341–348. https://doi.org/10.1007/s00374-018-1263-z

Wang L, O'Connor D, Rinklebe J, Sik Ok Y, Tsang DCW, Shen Z, Hou D (2020) Biochar aging: mechanisms, physicochemical changes, assessment, and implications for field applications. Environ Sci Technol 54:14797–14814. https://doi.org/10.1021/acs.est.0c04033

Wang A, Li X, Hao X, Luo X, Chen W, Huang Q (2022) Ammonia level influences the assembly of dissimilatory nitrate reduction to ammonia bacterial community in soils under different heavy metal remediation treatments. Sci Total Environ 838:156393. https://doi.org/10.1016/j.scitotenv.2022.156393

Wei Z, Senbayram M, Zhao X, Li C, Jin K, Wu M, Mizanur Rahman M, Shan J, Yan X (2022) Biochar amendment alters the partitioning of nitrate reduction by significantly enhancing DNRA in a paddy field. Biochar 4:44. https://doi.org/10.1007/s42773-022-00166-x

Wei Z, Li C, Ma X, Ma S, Han Z, Yan X, Shan J (2023) Biochar mitigates N_2O emissions by promoting complete denitrification in acidic and alkaline paddy soils. Eur J Soil Sci 74(6):e13428. https://doi.org/10.1111/ejss.13428

Wu L, Zheng H, Wang X (2021) Effects of soil amendments on fractions and stability of soil organic matter in saline-alkaline paddy. J Environ Manage 294:112993. https://doi.org/10.1016/j.jenvman.2021.112993

Xi D, Bai R, Zhang L, Fang Y (2016) Contribution of anammox to nitrogen removal in two temperate forest soils. Appl Environ Microb 82:4602–4612. https://doi.org/10.1128/aem.00888-16

Yang Q, Gong L, Zhang X, Zhang G, Wang L (2025a) The effect of arable land management on the reaction of anaerobic ammonium oxidation (anammox): a meta-analysis. Agronomy 15:466. https://doi.org/10.3390/agronomy15020466

Yang Q, Li H, Gong L, Zhang X, Wang L (2025b) Dissimilatory nitrate reduction to ammonium (DNRA) and *nrfA* gene in crop soils: a meta-analysis of cropland management effects. Glob Change Biol Bioenergy 17:e70039. https://doi.org/10.1111/gcbb.70039

Yin G, Hou L, Liu M, Li X, Zheng Y, Gao J, Lin X (2017) DNRA in intertidal sediments of the Yangtze Estuary. J Geophys Res-Biogeo 122:1988–1998. https://doi.org/10.1016/j.watres.2022.118381

Yoon S, Cruz-Garcia C, Sanford R, Ritalahti KM, Loffler FE (2015) Denitrification versus respiratory ammonification: environmental controls of two competing dissimilatory NO_3^-/NO_2^- reduction pathways in *Shewanella loihica* strain PV-4. ISME J 9:1093–1104. https://doi.org/10.1038/ismej.2014.201

Yuan Y, Bolan N, Prévoteau A, Vithanage M, Biswas JK, Ok YS, Wang H (2017) Applications of biochar in redox-mediated reactions. Bioresource Technol 246:271–281. https://doi.org/10.1016/j.biortech.2017.06.154

Yuan D, Wang G, Hu C, Zhou S, Clough TJ, Wrage-Mönnig N, Luo J, Qin S (2022) Electron shuttle potential of biochar promotes dissimilatory nitrate reduction to ammonium in paddy soil. Soil Biol Biochem 172:108760. https://doi.org/10.1016/j.soilbio.2022.108760

Zhang S, Zhang G, Wu M, Wang D, Liu Q (2021) Straw return and low N addition modify the partitioning of dissimilatory nitrate reduction by increasing conversion to ammonium in paddy fields. Soil Biol Biochem 162:108425. https://doi.org/10.1016/j.soilbio.2021.108425

Zhang L, Jiang M, Zhou S (2022a) Conversion of nitrogen and carbon in enriched paddy soil by denitrification coupled with anammox in a bioelectrochemical system. Environ Sci Technol 111:197–207. https://doi.org/10.1016/j.jes.2021.03.033

Zhang Y, Zhao H, Hu W, Wang Y, Zhang H, Zhou X, Fei J, Luo G (2022b) Understanding how reed-biochar application mitigates nitrogen losses in paddy soil: insight into microbially-driven nitrogen dynamics. Chemosphere 295:133904. https://doi.org/10.1016/j.chemosphere.2022.133904

Zhang L, Chen Z, Zhu S, Li S, Wei C (2023) Effects of biochar on anaerobic treatment systems: some perspectives. Bioresource Technol 367:128226. https://doi.org/10.1016/j.biortech.2022.128226

Zhang X, Zhou Q, Wang L, Wan B, Yang Q (2024) How biochar addition affects denitrification and the microbial electron transport system (ETSA): a meta-analysis based on a global scale. Agriculture 14:2320. https://doi.org/10.3390/agriculture14122320

Zhao Z, Cao Y, Li S, Zhang Y (2021) Effects of biowaste-derived biochar on the electron transport efficiency during anaerobic acid orange 7 removal. Bioresource Technol 320:124295. https://doi.org/10.1016/j.biortech.2020.124295

Zhou G, Yang X, Li H, Marshall CW, Zheng B, Yan Y, Su J, Zhu Y (2016) Electron shuttles enhance anaerobic ammonium oxidation coupled to iron (III) reduction. Environ Sci Technol 50:9298–9307. https://doi.org/10.1021/acs.est.6b02077